

Modeling Water Adsorption and Retention of Building Materials From Pore Size Distribution

Abdelkrim Trabelsi^{1,*}, Zakaria Slimani¹, Akli Younsi², Joseph Virgone¹ and Rafik Belarbi²

¹Univ Lyon, CNRS, INSA-Lyon, Université Claude Bernard Lyon 1, CETHIL UMR5008, F-69621, Villeurbanne, France.

²University of La Rochelle, CNRS, LaSIE, UMR-7356, Avenue Michel Crépeau, 17042 La Rochelle Cedex 1, France.

*Corresponding Author: Abdelkrim Trabelsi. Email: abdelkrim.trabelsi@univ-lyon1.fr.

Abstract: Water adsorption and capillarity are key phenomena involved during heat and moisture transfer in porous building materials. They account for interaction between solid matrix, liquid water and moist air. They are considered through Water Vapor Adsorption Isotherm (WVAI) and Retention Curve (RC) functions which are constitutive laws characterizing water activity within a porous medium. The objective of this paper is to present a water vapor adsorption and retention models built from multimodal Pore Size Distribution Function (PSDF) and to see how its parameters modify moisture storage for hygroscopic and near saturation ranges. The microstructure of the porous medium is represented statistically by a bundle of tortuous parallel pores through its PSDF. Firstly, the influence of contact angle and temperature on storage properties were investigated. Secondly, a parametric study was performed to see the influence of the PSDF shape on storage properties. Three cases were studied considering the number of modalities, the weight of each modality and the dispersion around mean radius. Finally, as a validation, the proposed model for WVAI were compared to existing model from literature showing a good agreement. This study showed that the proposed models are capable to reproduce various shapes of storage functions. It also highlighted the link between microstructure and adsorption-retention phenomena.

Keywords: Water vapor adsorption; capillarity; pore size distribution; WVAI and RC modeling; porous building materials

1 Introduction

The study of hygrothermal transfer in porous building materials is an important subject because it concerns several issues: materials durability, indoor air quality and energy. For instance, the cement-based building materials are very sensitive to the hygrothermal exchanges with the surrounding environment. These interactions with the ambiance can affect the hydration kinetics of the materials at early age and modify their properties and performances, especially their durability [1]. Moreover, the interactions can directly govern the durability, such as chlorides and carbonation attacks [2]. Moisture presence can considerably affect thermal gains or losses in buildings with direct relation to the energy consumption and mold growth especially in corners [3]. The condensed water in cold part of the envelope increases heat loss and enables mold growth deteriorating indoor air quality. Conversely, the use of high buffering capacity building envelope is a very efficient way to reduce the amplitude of daily moisture variations. It reduces heat loss due to air exchange if high buffering capacity envelope is used together with a humidity-controlled ventilation [4]. One of the key phenomena defining hygrothermal transfer in porous media is water vapor adsorption and retention.

Modeling these two phenomena is usually realized through nonphysical modeling using polynomial interpolation function minimizing the discrepancy to experimental data [5], or physical models like BET

model [6] where the parameters have physical significance. These models still require experimental data to identify their parameters.

Most of the studies addressed these phenomena through:

- the characterization of a material and its evolution [7-11]
- the modeling for a given material and the comparison between materials [12-16]
- the assessment of the impact of that properties on the whole heat and moisture transfer [4,17]

However, the literature on water vapor adsorption and retention modeling does not yet provide studies that link these two phenomena to the material microstructure. Therefore, in this paper, we will present a Water Vapor Adsorption Isotherm (WVAI) model and a Retention Curve (RC) model built from Pore Size Distribution Function (PSDF). The purpose of this approach is to show the impact of microstructure on water storage. In this way, we open the possibility to a material optimization process. The microstructure is represented statistically by a bundle of tortuous parallel pores where size distribution is a sum of Gaussian laws. In a second step, the water adsorption and retention physics are defined in this medium. It is based on equilibrium well known and widely used Jurin's and Kelvin's laws. Finally, a parametric study is realized changing the shape of the PSDF.

2 Method

PSDF can be derived from gas adsorption isotherm (usually nitrogen) to characterize a porous material [18]. This approach, more often used in chemistry, falls within a process where the aim is to describe the microstructure and not to see how microstructure affects adsorption phenomenon. In this work, we propose an inverse progress to go from microstructure characteristics toward adsorption phenomena and condensation to see how microstructure changes the behavior of porous media. We focus particularly on WVAI and RC.

The adopted method is represented in Fig. 1. The first step to consider is the construction of the PSDF. The obvious representation of pore size distribution is to assume the existence of few main pores with a dispersion around. In that respect, we defined the multimodal PSDF as a sum of weighted gaussian laws $w_i \cdot \mathcal{N}_i(r_i^{log}, \sigma_i^2)$ as per Eq. (1). Each modality is defined as a function of the mean radius r_i^{log} (with $r^{log} = \log r$, where r is the pore radius [m]), the standard deviation σ_i and the weight w_i . Associated cumulative function is given by Eq. (2).

$$f(r^{log}) = \sum_{i=1}^n \frac{w_i}{\sigma_i \sqrt{2\pi}} \times \exp \left[-\frac{1}{2} \left(\frac{r^{log} - r_i^{log}}{\sigma_i} \right)^2 \right] \quad (1)$$

$$F(r^{log}) = \sum_{i=1}^n \frac{w_i}{2} \left[1 + \operatorname{erf} \left(\frac{r^{log} - r_i^{log}}{\sigma_i \sqrt{2}} \right) \right] \quad (2)$$

Adopted representation for the description of the microstructure is a bundle of tortuous parallel pores with a porosity ε [m³/m³], a tortuosity τ [-] and a pore size distribution function f [-] (Eq. (1)). When relative humidity increases, water vapor is adsorbed by the solid matrix of the porous media and pores are filled until having capillary bridges. Pores are filled from the smallest to the biggest one. Thus, the cumulative function F [-] associated to the PSDF represents the ratio between volumetric water content θ_l [m³/m³] and the porosity (Eq. (3)).

$$F = \frac{\theta_l}{\varepsilon} \quad (3)$$

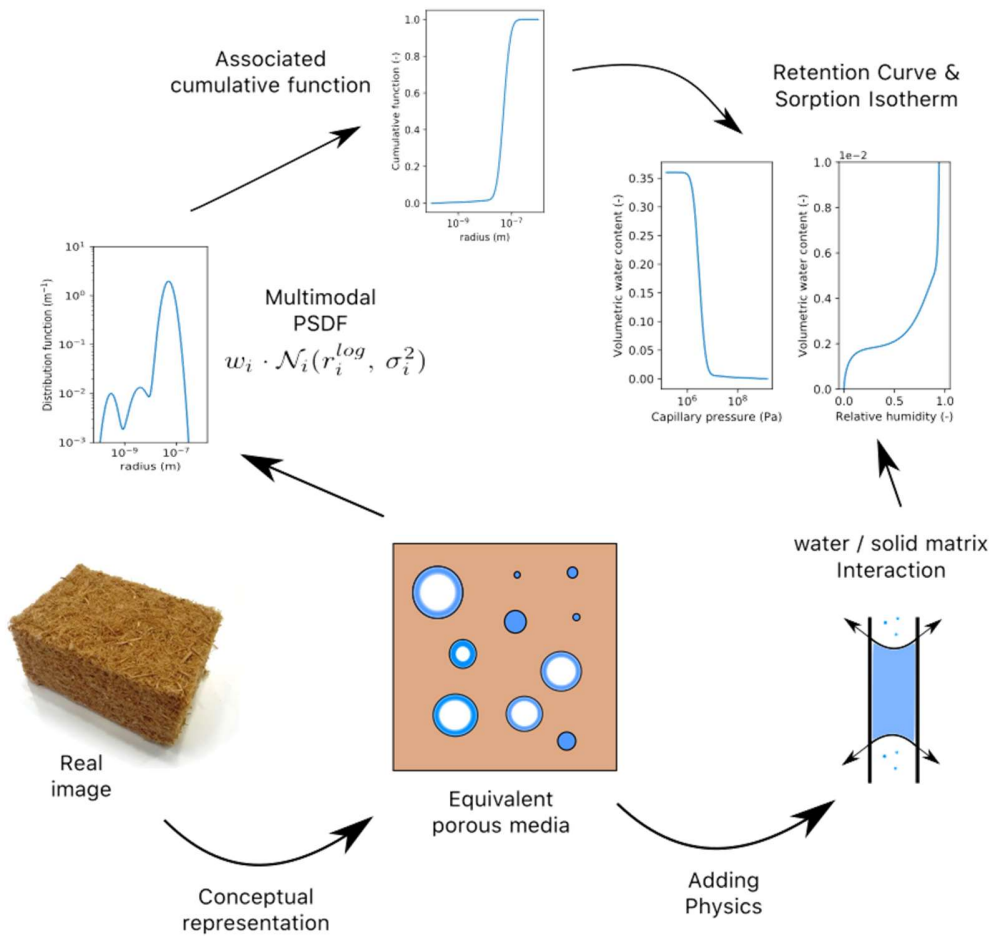


Figure 1: Schematic representation of the developed method

To build the WVAI and RC curves, we assume Jurin and Kelvin laws (Eqs. (4) and (5)) that allow to link geometrical parameters to physical parameters. The first equation gives a relationship between capillary pressure p_c [Pa], curvature and shape of the water-gas interface and finally surface tension. The second equation expresses the relationship between capillary pressure and relative humidity (rh [-]) at thermodynamic equilibrium. Finally, we assume that the Kelvin's radius is supposed equal to the pore radius. The Jurin's law is valid for capillaries where the cross section is circular [19]. Further equations should be considered if the shape is different. The Kelvin's law is widely used as a constitutive law for modeling heat and mass transfer under the assumption of local equilibrium [20].

$$p_c = \frac{2\gamma}{r} \cos \theta \tag{4}$$

$$p_c = -r_v T \rho_l \ln(\text{rh}) \tag{5}$$

For a given temperature T [K], the main parameters influencing capillary pressure and relative humidity of air in pores are radius r [m], contact angle θ [rad] and surface tension γ [N/m] whose common value for water is equal to 0.0728 N/m (r_v [J/kg/K] and ρ_l [kg/m³] are respectively the specific constant and density of water). Finally, we give a new mathematical formulation expressing retention and adsorption curves (Eqs. (6) and (7)) depending on physical and geometrical parameters:

$$\theta_i(p_c) = \varepsilon \sum_{i=1}^n \frac{w_i}{2} \left[1 + \operatorname{erf} \left(\frac{\log_{10} \left(\frac{2\gamma \cos \theta}{p_c} \right) - r_i^{\log}}{\sigma_i \sqrt{2}} \right) \right] \quad (6)$$

$$\theta_i(\text{rh}) = \varepsilon \sum_{i=1}^n \frac{w_i}{2} \left[1 + \operatorname{erf} \left(\frac{\log_{10} \left(-\frac{2\gamma \cos \theta}{r_v T \rho_l \ln(\text{rh})} \right) - r_i^{\log}}{\sigma_i \sqrt{2}} \right) \right] \quad (7)$$

3 Results and Discussion

3.1 Influence of the Contact Angle

Contact angle presents a hysteresis with a value varying according to solid matrix composition. In the literature, there is very little data available on this characteristic, as such, a parametric study is performed to see how contact angle affects WVAI and RC. Fig. 2 presents the variation of capillary pressure and relative humidity as a function of pore radius for different contact angles. Contact angle affects capillary pressure and relative humidity mainly for micropores and mesopores (radius less than 50 nm). In that range of porosity, when the meniscus curvature increases the capillary pressure goes down and the relative humidity goes up. For water, the commonly used value contact angle is equal to 0 radian. Moreover, as shown in Fig. 2 on the right, pores determining adsorption isotherm shape in the hygroscopic domain ($\text{rh} < 0.98$) are those less than 50 nm. In the next section, the contact angle is taken constant (equal to 0 rad). Thus, hysteresis effects are not considered. Further investigations should be performed on that parameter.

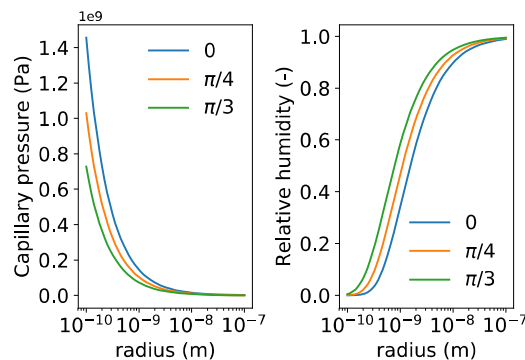


Figure 2: Evolution of capillary pressure and relative humidity as a function of the pore radius for different contact angles

3.2 Influence of the Temperature

The influence of temperature has been assessed only on thermodynamic equilibrium expressed by Kelvin's law. The impact of temperature due to the dependency of contact angle and surface tension has not been investigated because literature lacks quantified information on the dependency of these parameters on temperature. In order to show the influence of temperature on WVAI Eq. (7) has been considered for Reference function shown in Tab. 1 at three levels of temperatures: 5, 20 and 95°C.

The Reference function describes a material with an open porosity of 30% with microstructural characteristics that could be encountered for a real Civil Engineering material such as bricks. Its PSDF is defined with three modalities: the first one is in the micropores range, the second one is in the mesopores range and the last one is at the boundary between mesopores and macropores range. As a reminder, the International Union of Pure and Applied Chemistry [21] gave a classification of porous materials according to their pore diameter D as following:

-Micropores: $D < 2 \text{ nm}$

-Mesopores: $2 \text{ nm} \leq D \leq 50 \text{ nm}$

-Macropores: $D > 50 \text{ nm}$

We can see in Fig. 3 that the proposed model is able to reproduce a well-known observation on the dependency of WVAI on temperature. Indeed, for a given relative humidity, the moisture capacity, and the equilibrium moisture content increases as temperature decreases [13,22,23]. The difference between the three curves is small, it is higher for relative humidity less than 20% or greater than 50% while for the relative humidity in-between the moisture capacity is almost unaffected. This result corroborates the study from Zhang et al. [24].

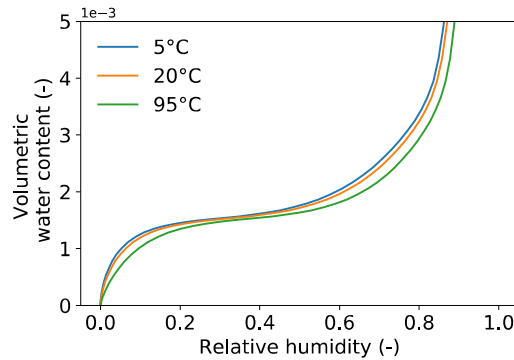


Figure 3: Effects of temperature on WVAI

3.3 Influence of the Parameters of the PSDF

In this section, let us assess the RC and WVAI represented using Eqs. (6) and (7) respectively. In order to evaluate the impact of PSDF on water storage functions, three cases were considered according to the triplet weight, mean radius and standard deviation: (w_i, r_i, σ_i) . The first case assesses the number of modalities, the second one the weight of each modality and the third one the dispersion around modalities. Studied functions parameters and their labels are displayed in Tab. 1.

Table 1: Studied cases

| Case | Modality 1 | Modality 2 | Modality 3 | Label |
|------|----------------------|------------------|---------------------|---------------------|
| 1 | (0.005, 0.3e-9, 0.2) | (0.1, 4e-9, 0.3) | (0.985, 25e-9, 0.2) | Reference |
| | likewise reference | deleted | likewise reference | 2 Modes |
| 2 | $w_1 = 1/3$ | $w_2 = 1/3$ | $w_3 = 1/3$ | Balanced |
| | $w_1 = 0.985$ | $w_2 = 0.1$ | $w_3 = 5e-3$ | Micropores dominant |
| 3 | $\sigma_1 = 0.3$ | $\sigma_2 = 0.5$ | $\sigma_3 = 0.3$ | Dispersed |
| | $\sigma_1 = 0.1$ | $\sigma_2 = 0.1$ | $\sigma_3 = 0.1$ | Restricted |

For case 1, the “Reference function” is compared to “2 Modes function” where the intermediate mode with a mean radius in the mesopores range has been deleted. For both functions the dominant mode is the third one corresponding to a macro-porous material. As a consequence, cumulative function and RC for both functions are almost same within a wide range of radius and capillary pressure (see Fig. 4). If we make a zoom in the hygroscopic range for the WVAI, we can see that for the 2 modes function, there is a plateau between 25 and 80% for which the water content does not vary although a variation in relative humidity. Compared to Reference case, the noticed plateau is due to the lack of mesopores that are determinant for

the adsorption behavior within the hygroscopic range. Fig. 4 shows that two modalities are not sufficient to describe correctly the sorption isotherm for macro-porous material. At least, three modalities as per Reference function is suited to give a variety in the pore size distribution.

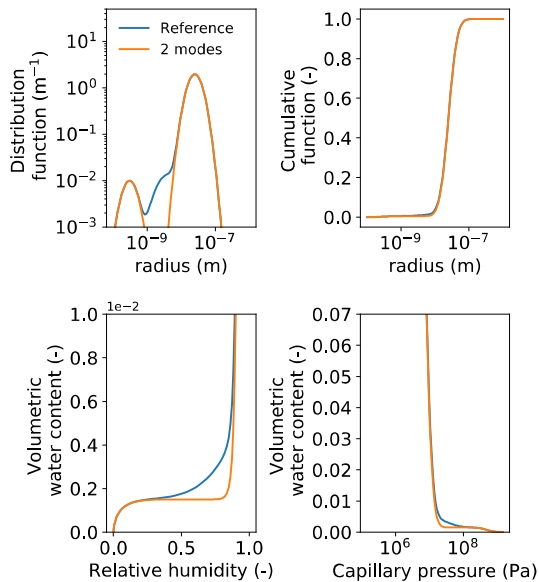


Figure 4: PSDF and associated Cumulative Function, WVAI and RC for case 1

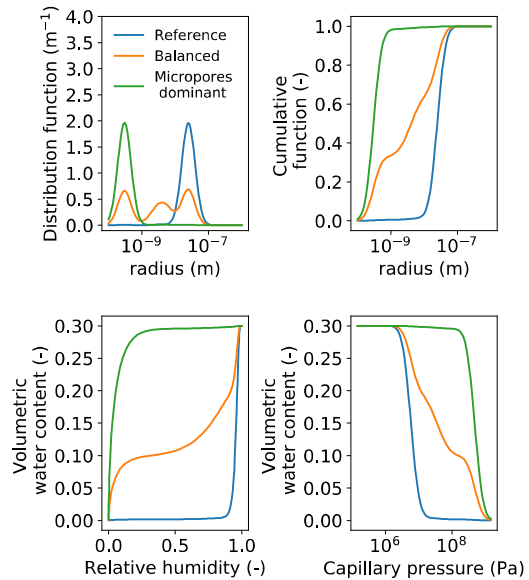


Figure 5: PSDF and associated Cumulative Function, WVAI and RC for case 2

For case 2, we compared three different PSDF and associated Cumulative Function, WVAI and RC: Reference, Balanced and Micropores dominant. The Reference one (macropores dominant) are suited for construction materials with a very low adsorption in the hygroscopic range (brick, polystyrene...). The balanced PSDF are suited for materials such as concrete with a large variety of pore size distribution including mesopores. The micropores dominant PSDF is not very common for building construction materials. As we can see in Fig. 5, this case shows the comparison of clearly distinguished functions. Compared to the two other functions, the balanced one shows the three stages in both the cumulative function and RC. For such a material, capillary movement are not negligible even in the hygroscopic range. For the reference case, although the existence of adsorption in the hygroscopic range, the adsorbed water remains very small compared to the water content at saturation. The adsorption for micropores dominant materials happens at low range of relative humidity until all pores filled. Case 2 shows that the weight of modalities defining the PSDF has a great importance in the final behavior of the material because it allows to exhibit the dominant behavior due to a dominant mode (micropores, macropores) or a behavior resulting from a balanced PSDF.

The last investigated parameter is the dispersion (see Fig. 6). It plays an important role in the slope of water storage functions (RC and WWSI). For relative humidity ranging from 20% to 60% the slope varies from 0 to a highest value for the most dispersed material. Consequently, it is determinant in the hydric inertia of the material and its Moisture Buffer Value (MBV). For the restricted case, more modalities should be added to have a smooth slope. Case 3 shows that the dispersed function allows more adsorption in the hygroscopic range (See WVAI) The restricted one could be used to model multi-stage adsorption materials belonging to type IV, V or VI according to the IUPAC adsorption isotherms classification.

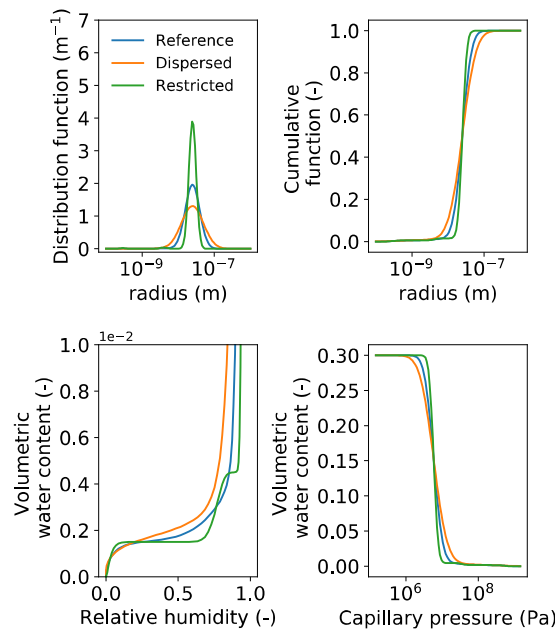


Figure 6: PSDF and associated Cumulative Function, WVAI and RC for case 3

3.4 Comparison to GAB Model

This part presents the comparison between the proposed model (Eq. (7)) and the well-known GAB model (Eq. (8)) for the representation of the WVAI of a Medium Density Fiberboard (MDF). This material has been chosen as the reference material in the framework of the numerical benchmark developed during the ANR HYGRO-BAT project [25,26]. It is the result of existing databases on the hygrothermal properties of construction materials. Its dry density ρ_s is equal to 589 kg/m³ and porosity ε is equal to 54.5%.

The GAB (Guggenheim-Anderson-de Boer) model is based on Langmuir’s theory and is distinguished by the fact that several layers can be superposed on the first adsorbed layer. It is used in several disciplines, notably agro-foodstuffs, chemical engineering and civil engineering [15,23,27].

$$\frac{\rho^m}{\rho_s} = \frac{m \times C \times K \times rh}{(1 - K \times rh)(1 + K(C - 1)rh)} \tag{8}$$

where ρ^m is the moisture content [kg/m³], m is the capacity of the first layer, C is a kinematic constant linked to the adsorption of the first layer and K is a kinetic constant linked to multimolecular adsorption.

Fig. 7 shows the experimental data and the associated MDF isotherm sorption model. For the comparison, water content in GAB model has been converted to volumetric water content. The parameters presented in Tab. 2 have been determined using non-linear least squares method minimizing the squared error between experimental data and predicted data from models. WVAI of the MDF belongs to type II according to the IUPAC adsorption isotherm classification. The material shows weak adsorption at low relative humidity with a monolayer capacity of 28 g_v/kg_s. It is a good hygroscopic material that adsorbs more than 36 kg/m³ of water at 60% relative humidity. The moisture content at saturation is about 545 kg/m³.

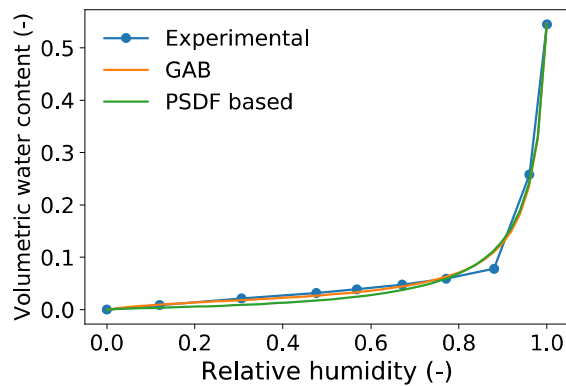


Figure 7: MDF water vapor sorption isotherm

The estimated parameters for the GAB model agree with those estimated by Hartely et al. [28] for same product family. Concerning PSDF based model, only one modality was sufficient to well reproduce the WVAI of the material. The mean radius is around 33.2 nm with a wide dispersion around. The material covers a wide range of pores including mesopores which explains its hygroscopicity. The coefficient of determination for the GAB model ($R^2 = 0.994$) is slightly higher than the PSDF model ($R^2 = 0.992$), nevertheless the approximation remains very good for both models.

Table 2: Models parameters

| GAB Model | | PSDF Model | | |
|-----------|-------|------------|----------------------|----------|
| m | C | K | r | σ |
| 0.028 | 8.077 | 0.9699 | $3.32 \cdot 10^{-8}$ | 0.73 |

4 Conclusion

In this paper, we presented a WVAI and RC models based on a probabilistic description of pore size distribution. The PSDF based models are capable to reproduce various shapes of WVAI and to explain link between microstructure and adsorption phenomenon. In the hygroscopic range, the micropores are responsible for adsorption for relative humidity lower than 60% and the mesopores for relative humidity higher. The proposed model WVAI was used to reproduce MDF sorption isotherm. It was compared to experimental data and GAB model. Good agreement was found. The proposed method could be used for material optimization. As future work, more research should be done to investigate contact angle and surface tension for different materials. In addition to that, more materials should be studied in different fields like agro-foodstuffs, chemical engineering and civil engineering to confirm the agreement of the proposed models.

References

1. Younsi, A., Bordy, A., Aggoun, S., Fiorio, B. (2018). Hydration-drying interactions in OPC pastes blended with recycled OPC paste fine powder: critical curing relative humidity hampering hydration. *Construction and Building Materials*, 90, 403-413.
2. Achour, M., Amiri, O., Bignonnet, F., Rozière, E. (2018). Numerical study of the effect of moisture on chloride and carbon dioxide transport in concrete. *12th fib International PhD Symposium in Civil Engineering*, 1065-1070.
3. dos Santos, G. H., Mendes, N., Philippi, P. C. (2009). A building corner model for hygrothermal performance and mould growth risk analyses. *International Journal of Heat and Mass Transfer*, 52(21), 4862-4872.

4. Slimani, Z., Trabelsi, A., Virgone, J., Belarbi, R., Djedjig, R. (2015). Use of the buffering capacity of the building envelope for the reduction of the rate of air exchange. *Energy Procedia*, 78, 1531-1536.
5. Xi, Y., Bažant, Z. P., Jennings, H. M. (1994). Moisture diffusion in cementitious materials Adsorption isotherms. *Advanced Cement Based Materials*, 1(6), 248-257.
6. Brunauer, S., Emmett, P. H., Teller, E. (1938). Adsorption of gases in multimolecular layers. *Journal of the American Chemical Society*, 60(2), 309-319.
7. Baroghel-Bouny, V., Mainguy, M., Lassabatere, T., Coussy, O. (1999). Characterization and identification of equilibrium and transfer moisture properties for ordinary and high-performance cementitious materials. *Cement and Concrete Research*, 29(8), 1225-1238.
8. Espinosa, R. M., Franke, L. (2006). Influence of the age and drying process on pore structure and sorption isotherms of hardened cement paste. *Cement and Concrete Research*, 36(10), 1969-1984.
9. Baroghel-Bouny, V. (2007). Water vapour sorption experiments on hardened cementitious materials: Part I: essential tool for analysis of hygral behaviour and its relation to pore structure. *Cement and Concrete Research*, 37(3), 414-437.
10. Collet, F., Bart, M., Serres, L., Miriel, J. (2008). Porous structure and water vapour sorption of hemp-based materials. *Construction and Building Materials*, 22(6), 1271-1280.
11. Aït-Mokhtar, A., Belarbi, R., Benboudjema, F., Burlion, N., Caprad, B. et al. (2013). Experimental investigation of the variability of concrete durability properties. *Cement and Concrete Research*, 45, 21-36.
12. Carmeliet, J., Roels, S. (2002). Determination of the moisture capacity of porous building materials. *Journal of Thermal Envelope and Building Science*, 25(3), 209-237.
13. Arlabosse, P., Rodier, E., Ferrasse, J. H., Chavez, S., Lecomte, D. (2003). Comparison between static and dynamic methods for sorption isotherm measurements. *Drying Technology*, 21(3), 479-497.
14. Limousin, G., Gaudet, J. P., Charlet, L., Szenknect, S., Barthès, V. et al. (2007). Sorption isotherms: a review on physical bases, modeling and measurement. *Applied Geochemistry*, 22(2), 249-275.
15. Trabelsi, A., Belarbi, R., Turcry, P., Aït-Mokhtar, A. (2011). Water vapour desorption variability of in situ concrete and effects on drying simulations. *Magazine of Concrete Research*, 63(5), 333-342.
16. Zhang, Z., Thiéry, M., Baroghel-Bouny, V. (2014). A review and statistical study of existing hysteresis models for cementitious materials. *Cement and Concrete Research*, 57, 44-60.
17. Kwiatkowski, J., Woloszyn, M., Roux, J. J. (2009). Modelling of hysteresis influence on mass transfer in building materials. *Building and Environment*, 44(3), 633-642.
18. Rouquerol, F., Luciani, L., Lewellyn, P., Denoyel, R., Rouquerol, J. (2003). Texture des matériaux pulvérulents ou poreux. *Techniques de l'ingénieur*, 1-24.
19. Pradhan, B., Nagesh, M., Bhattacharjee, B. (2005). Prediction of the hydraulic diffusivity from pore size distribution of concrete. *Cement and Concrete Research*, 35(9), 1724-1733.
20. Tariku, F., Kumaran, K., Fazio, P. (2010). Transient model for coupled heat, air and moisture transfer through multilayered porous media. *International Journal of Heat and Mass Transfer*, 53(15-16), 3035-3044.
21. Sing, K. S. W., Everett, D. H., Haul, R. A. W., Moscou, L., Pierotti, R. A. et al. (1985). Reporting physisorption data for gas, solid systems with special reference to the determination of surface area and porosity (Recommendations 1984). *Pure and Applied Chemistry*, 57(4), 603-619.
22. Burgess, C. G. V., Everett, D. H., Nuttall, S. (1989). Adsorption hysteresis in porous materials. *Pure and Applied Chemistry*, 61(11), 1845-1852.
23. Furmaniak, S., Terzyk, A. P., Gauden, P. A. (2007). The general mechanism of water sorption on foodstuffs-Importance of the multitemperature fitting of data and the hierarchy of models. *Journal of Food Engineering*, 82(4), 528-535.
24. Zhang, X., Zillig, W., Künzler, H. M., Mitterer, C., Zhang, X. (2016). Combined effects of sorption hysteresis and its temperature dependency on wood materials and building enclosures-part II: hygrothermal modeling. *Building and Environment*, 106, 181-195.
25. Woloszyn, M. (2015). Vers une méthode de conception HYGRO-thermique des BATiments performants: démarche du projet HYGRO-BAT. *Les Modèles Face Aux Résultats Expérimentaux*, 1-8.

26. HYGRO-BAT (2015). Livrable de la Tâche 2.3: modélisation, simulations et confrontation avec l'expérimental. ANR-10-HABISOL-005-01.
27. Collet, F., Achchaq, F., Djellab, K., Marmoret, L., Beji, H. (2011). Water vapor properties of two hemp wools manufactured with different treatments. *Construction and Building Materials*, 25(2), 1079-1085.
28. Hartley, I. D., Wang, S., Zhang, Y. (2007). Water vapor sorption isotherm modeling of commercial oriented strand panel based on species groups and resin type. *Building and Environment*, 42(10), 3655-3659.